North American Precipitation and Temperature Patterns Associated with the El Niño/Southern Oscillation (ENSO)

C. F. ROPELEWSKI AND M. S. HALPERT

Climate Analysis Center/NMC/NWS/NOAA, Washington, DC 20233

(Manuscript received 3 March 1986, in final form 12 May 1986)

ABSTRACT

This paper describes an investigation of the "typical" North American precipitation and temperature patterns associated with the El Niño/Southern Oscillation (ENSO). Monthly surface temperature and precipitation data are analyzed using a method designed to identify regions of the globe that have responses associated with ENSO. Monthly composites, covering idealized two-year ENSO episodes, are computed for temperature and precipitation at all stations with data spanning seven or more ENSO events. The first harmonic is extracted from the 24 monthly composite values and plotted in the form of a two-year harmonic dial vector. When plotted on a map of North America, these vectors reveal both the regions of coherent response and the phase of the response with respect to the evolution of the ENSO episode. Time series of temperature and precipitation for the regions identified in the harmonic vector maps are examined to determine the magnitudes of the responses and the percentage of the time that the identified response actually occurred in association with the ENSO events. The temperature anomalies are expressed in terms of standardized departures, while precipitation departures are expressed as percentiles of the appropriate gamma distributions, fitted to the entire data record.

The analysis shows that above normal precipitation was associated with ENSO in 18 out of 22 cases (81%) in the "season" starting with October of the ENSO year to March of the following year for an area of North America that includes parts of the southeastern United States and northern Mexico. Above normal precipitation was also observed in the Great Basin area of the western United States in 9 out of 11 cases (81%) for the April through October "season" during ENSO years. No high latitude precipitation signals were indicated by this analysis. Areas of Alaska and western Canada experienced positive temperature anomalies in 17 out of 21 ENSO episodes (81%) during the "season" defined by December of the ENSO year through the following March. Parts of the southeastern United States near the Gulf of Mexico were found to have negative temperature anomalies associated with 20 out of 25 ENSO episodes (80%) for the "season" October of the ENSO year through the following March.

1. Introduction

The evolution of the El Niño/Southern Oscillation (ENSO) and corresponding anomalies in surface temperature and precipitation over the equatorial Pacific have been well described in the recent literature (e.g., Rasmusson and Carpenter, 1982). The relationships between midlatitude surface temperature and precipitation and ENSO are not so well documented. Suggestions of statistical links between the Southern Oscillation and surface parameters over North America date back to the pioneering studies of Walker (1924) and Walker and Bliss (1932). The diagnostic studies of Berlage (1966), as well as the more recent work of Douglas and Englehart (1981), Rasmusson and Wallace (1983), Rasmusson and Carpenter (1983), Shukla and Paolino (1983), Kousky et al. (1984), also provide evidence of links between ENSO and midlatitude temperature and precipitation. A midlatitude response to ENSO forcing is further supported by theoretical and modeling studies of the atmospheric circulation (Hoskins and Karoly, 1981; Opsteegh and Van den Dool, 1980; Webster, 1981; Blackmon et al., 1983), as well as statistically based circulation studies (Wallace and Gutzler, 1981; Horel and Wallace, 1981; Arkin, 1982).

The purpose of this paper, an extension of Ropelewski (1986), is to provide an improved description of the magnitude, phase, and geographical extent of ENSO-related response in temperature and precipitation over North America. We are particularly interested in defining those areas of the continent over which the ENSO response is both consistent and strong. The data used in this study are discussed in the next section. The analysis technique is described in section 3, and the results and conclusions are discussed in section 4.

2. Data

The analysis is based on monthly precipitation totals and monthly mean temperatures of surface meteorological station data in North America for the 1875–1980 period. Time series plots include data through the 1982/83 ENSO, but this episode was not included in the analysis to determine the typical ENSO-related response. The primary source of these data is the National Center for Atmospheric Research (NCAR)

World Monthly Surface Station Climatology, supplemented by the Local Climate Data (LCD) summaries for some locations in the United States. No attempts were made to correct for apparent biases or errors in the station data, but individual stations whose time series of temperature and precipitation exhibited clear biases or discontinuities were eliminated from the analysis. Stations with less than 30 years of data or spanning less than seven ENSO events were also excluded from the analysis. Stations with missing data for a month or "season" were excluded from the analysis for that particular month or season.

A more detailed analysis of precipitation in the United States was performed using the climatic division data (National Climatic Data Center, 1981). These data are spatial averages of observations from several cooperative sites within the 344 climate divisions and represent a dense network of continuous monthly precipitation data, but only for a period starting in January 1931 (e.g., see Janowiak et al., 1986). Since the precipitation for each climate division is formed from the averages of observations at several cooperative stations, as well as observations from the first-order stations for some divisions, these areal-averaged means represent a quasi-independent source of data for the analysis of precipitation over the United States.

3. Analysis

The analysis of the ENSO response in surface temperature and precipitation is especially difficult because 1) there are inhomogeneities in station records; 2) individual stations may be unrepresentative of the large scale, due to local effects; and 3) the magnitude and extent of the surface ENSO-related signal may vary from episode to episode.

In the first step of the analysis, we ranked the data for each individual month, normalized the rank by the total number of years of data, and expressed this ratio as a percent, or percentile rank, to minimize the problems enumerated above. Percentile ranks have been shown to provide a systematic way of dealing with the disparities among several stations and are particularly "robust" or immune from the biases that arise in other statistics because of extreme values in the sample distributions (Meisner, 1976).

Based on the events identified by Rasmusson and Carpenter (1983), ENSO composite ranks were formed for the two-year period starting with the July preceding the episode, designated as July(−) in this study. With this convention, the evolution of a typical, or composite, ENSO episode would be described by the appearance of positive sea surface temperature anomalies in December(−) with the maximum anomalies occurring during year(0). The 24-month series were subjected to a harmonic analysis that yields the amplitudes and phases of the first harmonic of the composite ENSO cycle (e.g., Fig. 1). This analysis is analogous to that used by Hsu and Wallace (1976) in their investigation of the annual cycle in precipitation; but in the current study, the phase of a 24-month harmonic des-

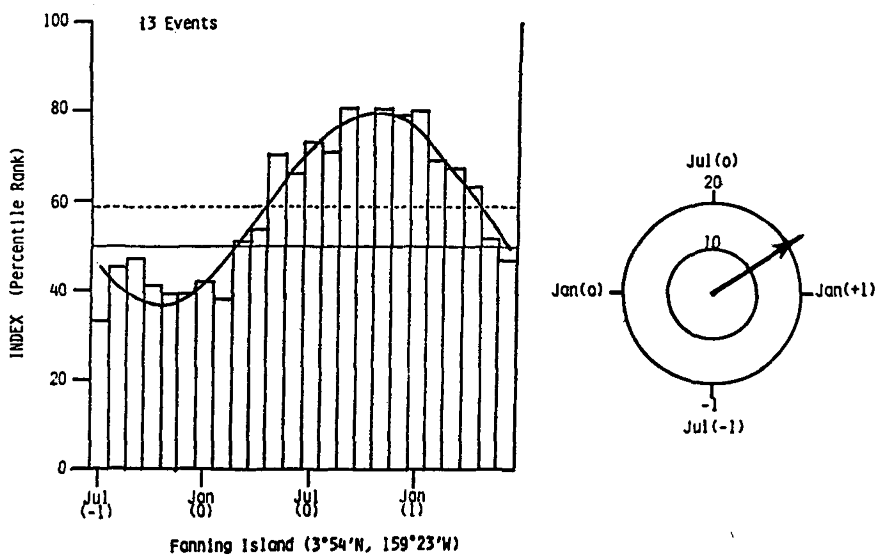

FIG. 1. Example of composite percentile ranks fitted by a 24-month harmonic. The index value for each month represents an average over 13 ENSO events in this example. The (−1, 0, +1) refer to months in the year previous, during and following an ENSO event in the Rasmusson and Carpenter (1983) convention. The year(0) months refer to months during the year in which maximum ENSO-related sea surface temperature anomalies generally occur in the east Pacific. The harmonic dial to the right illustrates the vector convention for displaying the amplitude and phase of the fitted harmonic. The months January and July are indicated as reference points on the harmonic dial.

ignates the time within the composite ENSO sequence when the monthly precipitation or temperature had the strongest apparent positive response. Plotting the harmonics as vectors on a map (Fig. 2) provides a method to subjectively identify candidate geographic areas that appear to have a coherent ENSO response. We attempted to choose the largest areas of coherent ENSO response, where the "coherence" is estimated through the computation of the ratio of the magnitude of the average vector, $[V]$, to the average of the individual vector magnitudes, S,

$$\text{Coherence} = \frac{[V]}{S}. \qquad (1)$$

The average vector, $[V]$, is constructed from the average of the individual components of the harmonic vectors within the region. The quantity S is simply the average of the individual vector magnitudes. The coherence is computed in precisely the same manner as the quantity often referred to in tropical meteorology as the "steadiness." The analysis that follows is limited to areas for which values of the coherence were equal to or greater than 0.80. This eliminates from the analysis regions that contain harmonic vectors with large amplitudes at a few stations which have little consistency in phase, i.e., low coherence.

The data for the stations within candidate areas were subjected to the following analysis:

1) Time series are formed for precipitation (temperature) based on the percentiles of the gamma (normal) distribution (Ropelewski et al., 1985) for stations or climate divisions within a region. Percentiles of the appropriate distribution are used to characterize precipitation and temperature for the remainder of the analysis since they represent quantities that are easier to interpret and relate to physical processes than the percentile ranks.

2) ENSO composites are formed for each station and averaged for all the stations within the regions. The resulting 24-month ENSO "aggregate" composite is plotted to identify a single "season" within the ENSO cycle with the largest apparent response.

3) Time series of the percentiles averaged for all stations within the area are plotted for the appropriate "season" defined in the previous step. The time series are examined for consistency of response associated with ENSO.

a. Precipitation

The map of the harmonic analysis vectors for station precipitation (Fig. 2) indicates four regions of North America that appear to have a coherent ENSO response. Three of the regions straddle the 40° parallel of latitude and from east to west on Fig. 2 are the Mid-Atlantic (MA), the High Plains (HP), and the Great

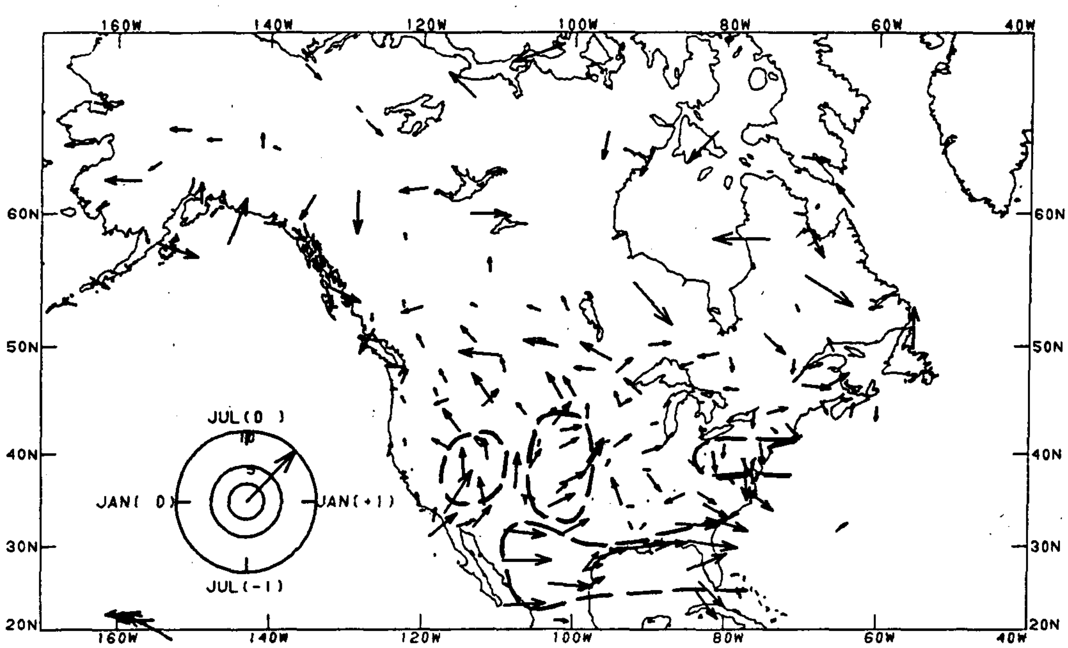

PREC INDEX WARM EPISODES 24 MONTH PERIOD

FIG. 2. Station vectors based on the 24-month harmonic fitted to ENSO precipitation composites. A minimum of seven ENSO events is represented by each vector. The outlined areas of "coherent" response, i.e., with coherence of at least 0.8, were selected for further analysis.

Basin (GB). A fourth region, the Gulf and Mexican Area (GM), lies to the southeast. Since all of the station precipitation areas except for the GM area are entirely within the United States, we repeated the analysis using the climate division areal-averaged precipitation data in order to have a check on the results. These climate-division-based harmonic dial vector plots, Fig. 3, show much greater data density and thus more spatial continuity than the station data, but they essentially delineate the same areas as defined in Fig. 2. A result of the greater data density is the appearance of an additional candidate area, the Pacific Northwest.

Composite precipitation percentiles for each region (Figs. 4a–e) indicate that the GM, GB, and HP regions may have an ENSO-related response. The percentile composites for the other candidate areas show no clearly defined single wet or dry "season" within the ENSO cycle and thus they are eliminated from further consideration in this analysis.

The time series of the October(0) to March(+) precipitation percentiles averaged over all stations in the GM region (Fig. 5) illustrates the remarkable consistency in the precipitation with respect to the ENSO in this part of North America. This "season" showed above normal, i.e., greater than the 50th percentile, precipitation for 18 out of 22 ENSO events. Further, of the nine occurrences of index values equal to or greater than the 70th percentile, eight of them occurred in association with ENSO. None of the occurrences in the lowest 30th percentile were associated with ENSO.

Time series of the GB region precipitation index based on the climate division data for the April(0) to October(0) season (Fig. 6a) shows above normal precipitation for 9 out of the 11 ENSO events since 1931. While the index shows values of greater than or equal to the 70th percentile for five of the ENSO years, positive values of the same magnitude or greater also occur during four non-ENSO-related years. None of the ENSO-related seasons in the Great Basin area fall into the lowest, or driest, 30th percentile. The time series of precipitation over the same region based on the station data (Fig. 6b) shows the same ENSO relationship over a slightly longer time period, 1922 to 1984. This time series indicates that 12 out of 14 ENSO April(0) to October(0) "seasons" were associated with above median precipitation.

Time series of the precipitation index for the HP region, April(0) to October(0) in Fig. 7a, shows an example of an inconclusive result. While 8 of the 11 ENSO seasons are associated with above median precipitation in the time series based on the climate division data, the longer time series—from 1875 to 1984—of station data over the same region (Fig. 7b) shows a much weaker ENSO relationship with only 16

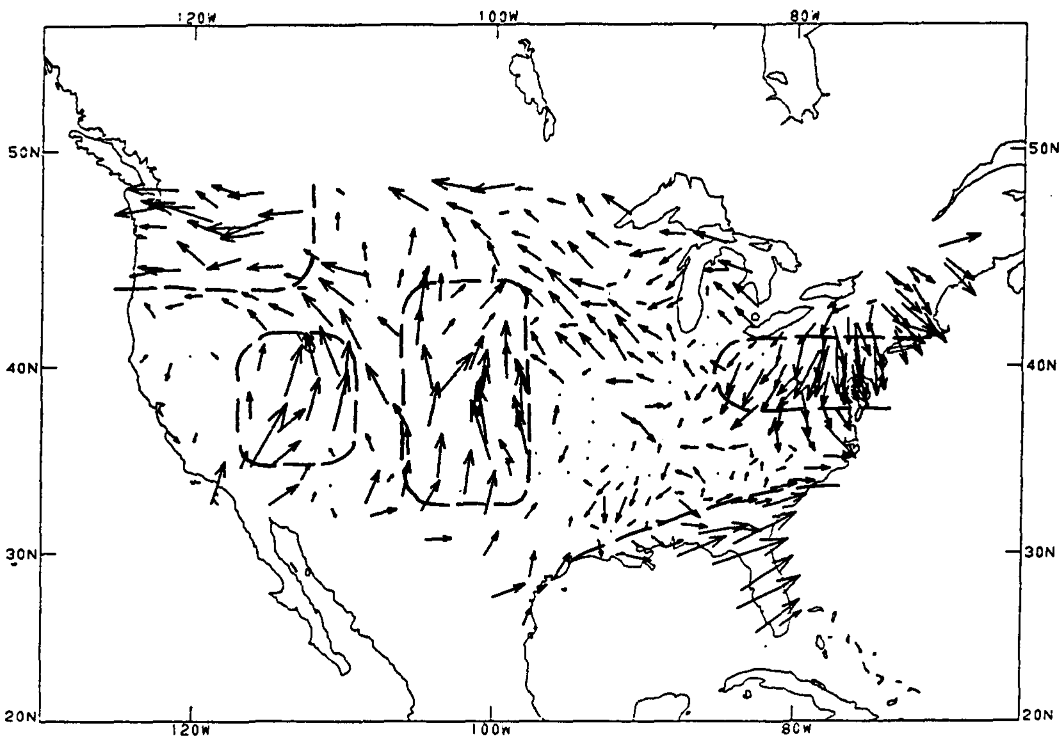

PREC INDEX WARM EPISODES 24 MONTH PERIOD

FIG. 3. As in Fig. 2 except based on the climate division data for the United States only.

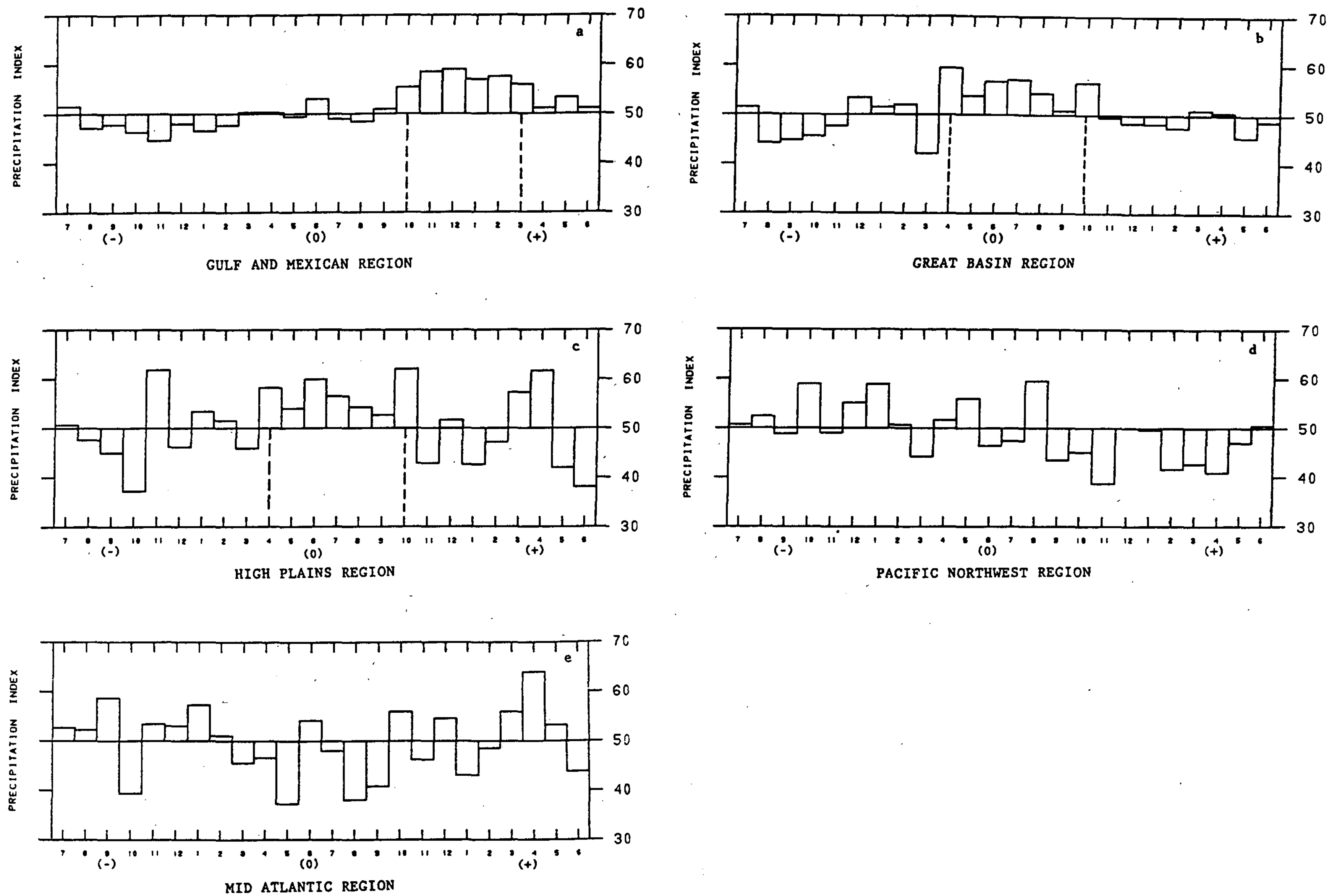

FIG. 4. ENSO composite precipitation percentiles for the (a) GM region, (b) GB region, (c) HP region, (d) PN region, and (e) MA region, outlined in Figs. 2 and 3. These composites are based on the average percentile precipitation for each of the stations in these areas. The dashed lines delineate the "season" of possible ENSO-related response. Composites run from the July before (−) the episode to the June following (+).

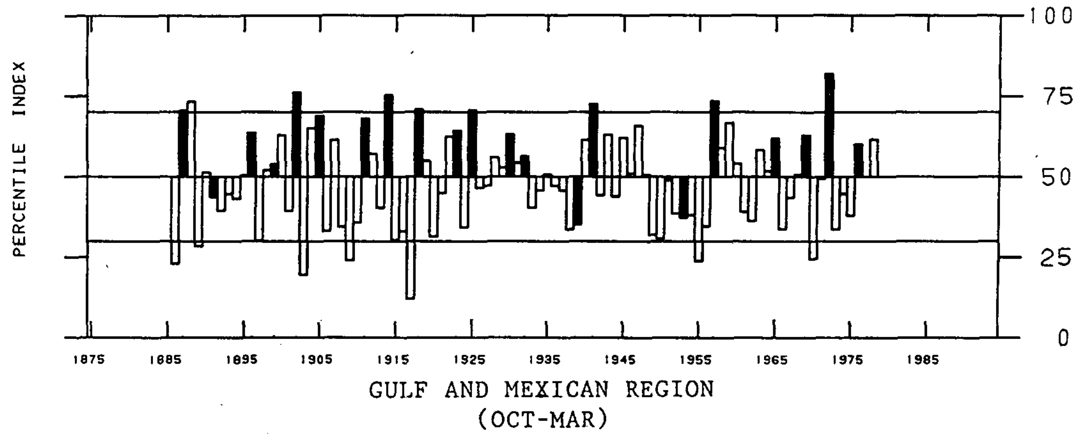

FIG. 5. Time series of the GM region, i.e., Gulf and Mexican, precipitation for the October(0) to March(+) season. Precipitation is represented by the average of the precipitation percentiles for each of the stations within the area; ENSO years are represented by the dark bars. Of the 22 ENSO episodes shown here, 18 are associated with above normal precipitation in the Gulf area.

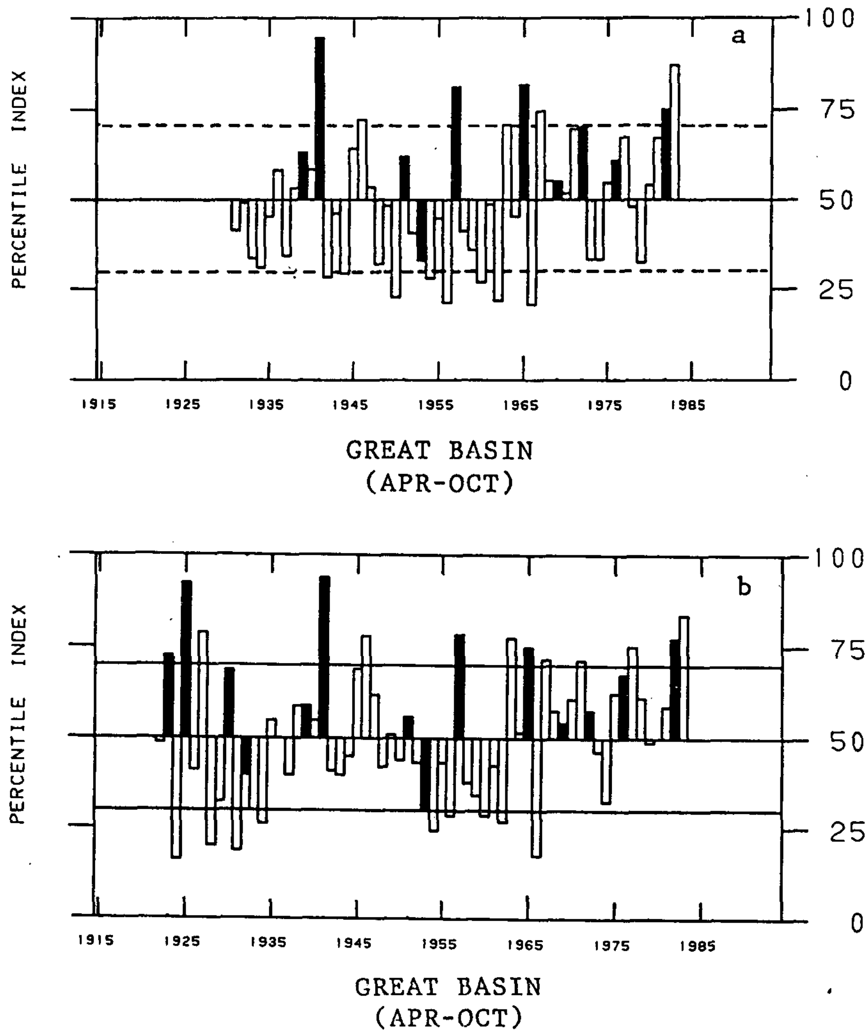

FIG. 6. As in Fig. 5 except in the Great Basin area for the April(0) to October(0) "season" based on (a) the climate division and (b) station precipitation. Of the 11 (14) ENSO episodes in the climate division (station) time series, 9 (12) were associated with above normal precipitation.

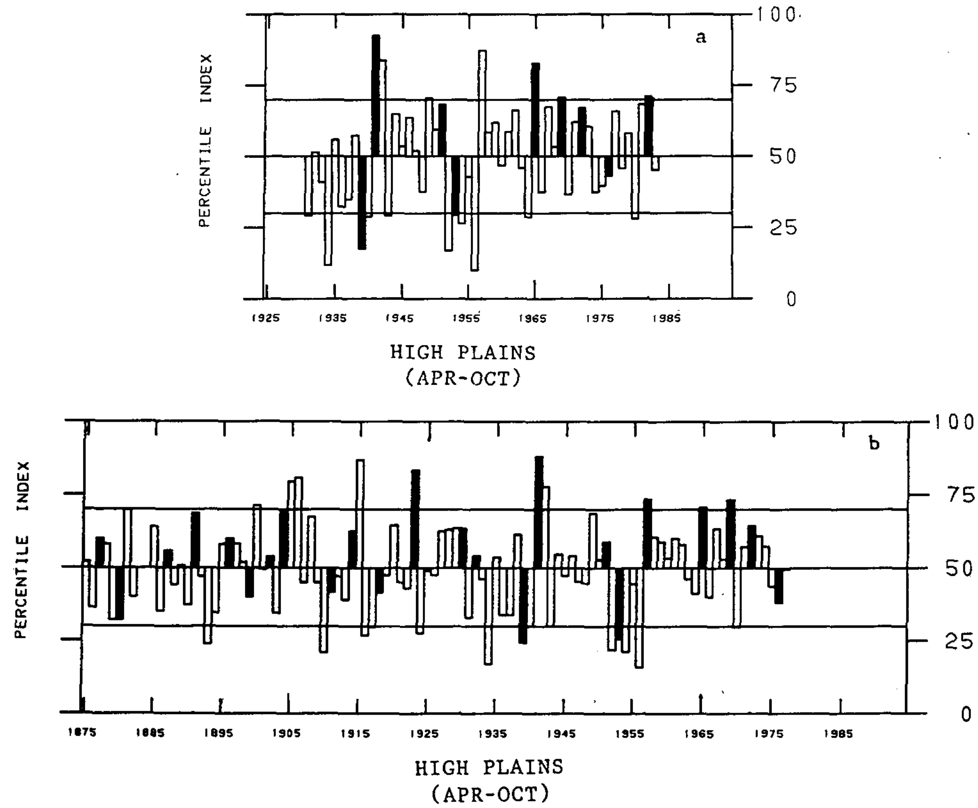

FIG. 7. As in Fig. 5 except for the High Plains region, based on (a) climate division data and (b) station data. A consistent ENSO-related response is not evident for this area.

of 24 ENSOs having above normal precipitation. The probability of getting 16 observations of the same sign strictly by chance is relatively high; i.e., the result is not significant at the fairly broad 90% level. The precipitation index exceeded the 70% index value with only five ENSO episodes, and two episodes were associated with values of less than 30%. Thus it does not appear that ENSO is a reliable discriminator of precipitation anomalies for the HP region.

b. Temperature

Similar analyses were performed on the station temperature data. The resulting map of harmonic dial vectors (Fig. 8) indicates coherent responses within the three outlined regions, Northwest North America (NNA), Southeast United States (SUS) and Eastern Canada (EC). El Niño/Southern Oscillation composites of standardized temperature for each of the regions (Figs. 9a–c) indicate that the NNA and SUS regions have well-defined "seasons" of potentially significant ENSO-related response, but the EC region does not.

Time series of the standardized temperature departures averaged over all stations in the NNA region for the December(0) to March(+) season (Fig. 10) show positive temperature departures for 17 out of 22 ENSO events in the period from 1890 to 1984. The index values equal or exceed 0.5 in 14 of the 22 ENSO years. If we assume that the index is normally distributed, then the 0.5 and −0.5 values correspond to the 70th and 30th percentiles of the distribution, respectively. Only one of the ENSO episodes, 1951, was associated with a negative temperature index value of less than −0.5.

In the SUS region the apparent ENSO-related temperature response occurs in roughly the same season, October(0) to March(+), as the temperature response in the NNA region and the precipitation response in the GM region, whose area is virtually coincident with SUS in the United States. The time series of station-averaged standardized temperature departures for this season (Fig. 11) shows negative departures for 20 out of 25 ENSO events in the 1880 to 1984 period. The magnitude of index values for the ENSO years equaled or exceeded −0.5 in 14 of the 25 ENSO years. Only one of the ENSO episodes, again 1951, is associated with a positive temperature index value of greater than +0.5 in this region.

The time series of temperature indices indicates a strong tendency for the temperature departures in NNA and SUS to be of opposite sign during ENSO years. This dichotomy in the phase of the response is also suggested in the plot of the harmonic dial vectors (Fig. 8). [Note that the convention in plotting the harmonic

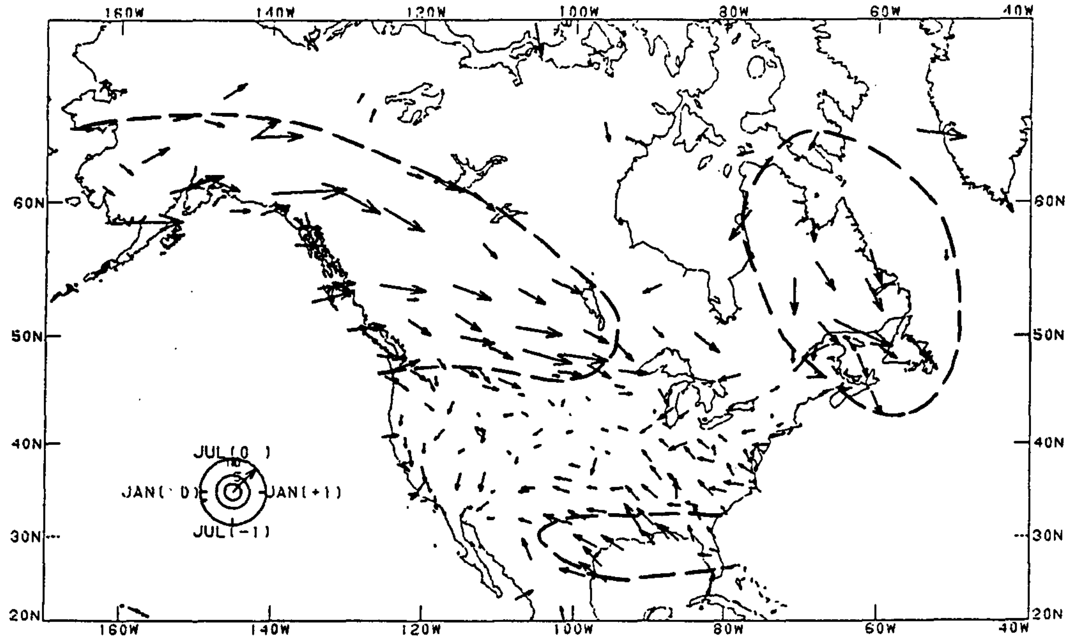

FIG. 8. As in Fig. 2 except for temperature.

dial vectors is that the arrow points to the positive side of the fitted harmonic, even though the signal of interest may be on the negative side. Thus, in the SUS, temperature harmonic vectors point toward the winter of the ENSO year, year(0) in our convention, but an examination of the ENSO composites in Fig. 9 and time series in Fig. 11 clearly shows that the principal signal occurs with the low temperatures in the following year.] The correlation between the NNA and SUS temperature indices for ENSO years (22 cases) is −0.68, while for non-ENSO years (70 cases) the correlation drops to −0.25. Allowing for the differences in sample size, the ENSO-year correlation is significant at greater than the 99.9% level, while the non-ENSO year relation just meets the 95% confidence level. Note that the significance levels quoted above are with respect to a biased sample and that unbiased significance values would be lower. There is no reason to suspect, however, that the relatively stronger correlation associated with ENSO would not hold with respect to unbiased statistics.

4. Summary and conclusions

Of the candidate regions indicated by the first step of the precipitation analysis, only the GM and GB areas showed a consistent ENSO-related precipitation signal; i.e., in both regions 81% of the ENSO cases experienced above normal precipitation (Table 1). The GM region showed positive precipitation departures for the October(0) to March(+) "season," and the GB regions showed positive departures for the April(0) to October(0) "season." Although there was some indication of an ENSO-related signal in the HP region, examination of the time series indicated that the ENSO response was not consistent. No other areas of North America showed a clear ENSO-related precipitation response. The lack of a consistent ENSO-related precipitation response at higher latitudes does not rule out the possibility of ENSO-related phenomena at these latitudes, but may be a reflection of the sensitivity of regional precipitation to the exact location and strength of ENSO-related PNA (Pacific–North America) or other circulation patterns. The response in the GM region is consistent with Douglas and Englehart (1981) and may be an indication of a more direct link to ENSO forcing than a "teleconnected" PNA pattern. Vigorous ENSO-related convection is typical in the equatorial Pacific, south of the GM region. This convection has been linked to stronger than normal westerlies in the Gulf of Mexico (e.g., 200 mb ENSO composites in Arkin, 1982) and, hence, a tendency for more frequent storms and precipitation in the Gulf. This possible direct link to the ENSO-related forcing may account for the consistency of the precipitation response in the GM region.

An explanation for the apparent ENSO-related signal in the GB area is more difficult to construct. The ENSO precipitation composite for this region (Fig. 4b) suggests that this apparent signal may be in phase with the bi-

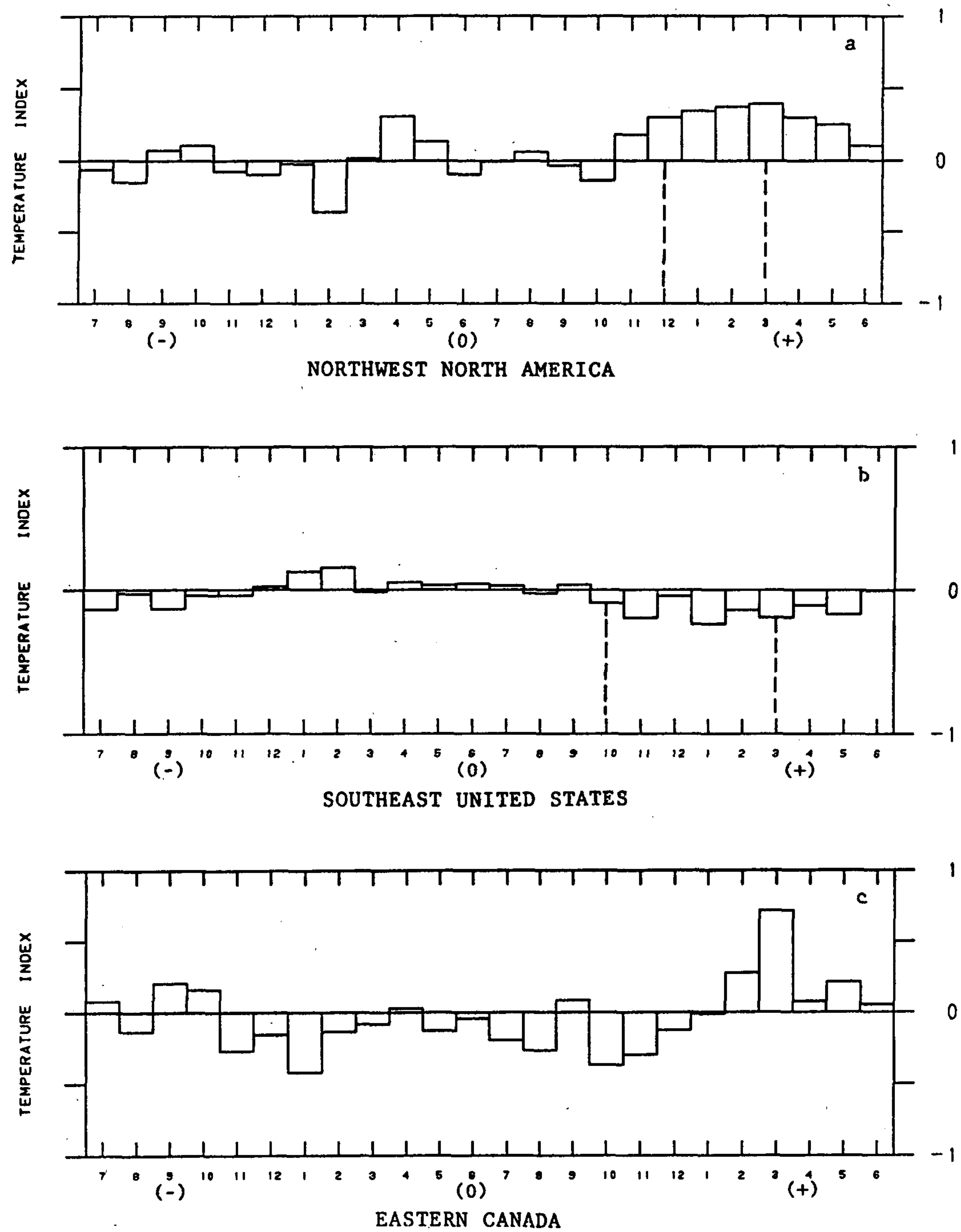

FIG. 9. ENSO composite standardized temperature for (a) northern North America (NNA), (b) southeastern United States (SUS), and (c) eastern Canada (EC). These composites are based on the average standardized temperature for each of the stations in the areas outlined in Fig. 8. The "season" of apparent ENSO-related response is indicated by dashed lines.

modal precipitation cycle typical in this part of the United States (Hsu and Wallace, 1976) and could represent an enhancement of this normal cycle. The physical mechanisms for the increased precipitation early in this "season," i.e., April(0) to June(0), and the persistence of this apparent signal through the northern summer are not clear. In a case study of the heavy precipitation over the United States associated with

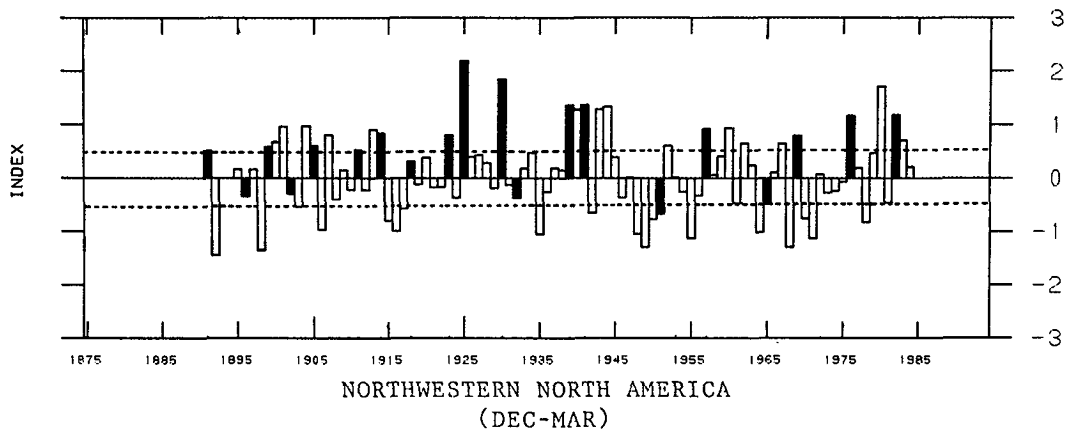

FIG. 10. Time series of average standardized temperatures for northwest North America in the December(0) to March(+) "season." This index is positive for 17 of 22 ENSO events.

the 1982/83 ENSO episode, Douglas and Englehart (1984) found that enhanced precipitation could be linked with the development of a midlatitude trough over the southwestern part of the country. Although positive sea surface temperature anomalies are not a normal ENSO-related feature in the Pacific west of Baja California this early in the ENSO cycle (Norton et al., 1985), the occurrence of warm water might help to increase precipitation amounts in this region.

Three candidate regions for temperature were identified, but only the NNA and SUS regions showed a clearly defined, consistent, ENSO-related temperature response in the composite indices. The tendency for above normal temperatures in Alaska and western Canada and below normal temperatures in the SUS is consistent with the anomalies expected with a PNA circulation pattern, i.e., low pressure in the Gulf of Alaska, a ridge over NNA, and a trough in the SUS. The PNA pattern has often been associated with ENSO, but its exact configuration varies from episode to episode. While the temperature anomalies at high latitudes may be relatively insensitive to small changes in the location of the PNA high pressure ridge, temperature anomalies at lower latitudes are more likely to respond to variations in the exact configuration of high and low pressure PNA centers. The exceptionally large negative correlations between the temperature in NNA and SUS during ENSO years as compared to non-ENSO years suggests that the PNA pattern tends to occur more often during ENSO years. The pattern of positive temperature anomalies in NNA and negative anomalies in the SUS occurs for 17 of the 21 episodes with data for both regions. The reverse anomaly pattern, negative anomalies in NNA, positive in the SUS, occurs in four of the remaining five episodes (1899, 1902, 1932, and 1951). Of these reverse pattern cases only the 1951 episode exhibited index values with magnitudes greater than 0.5, implying that the 1951 ENSO was far different—at least in its high latitude response—than the other ENSO episodes.

The differences between the patterns of temperature and precipitation response to ENSO in North America suggests that, while both are related to ENSO, the physical mechanisms responsible for these anomaly

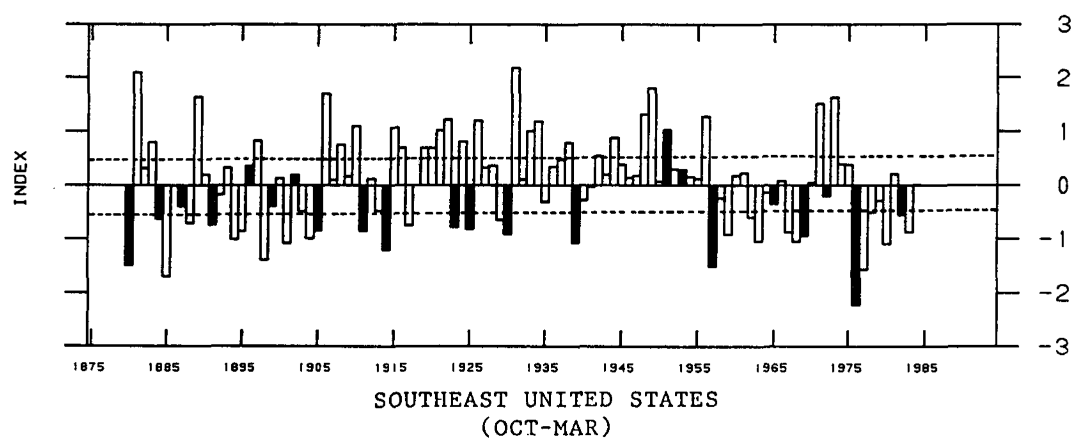

FIG. 11. As in Fig. 10 except for the SUS region October(0) to March(+) "season."

TABLE 1. Summary of ENSO-related precipitation and temperature response in North America. [The (0) notation refers to months of the ENSO year and the (+) notation to months of the year following ENSO. ENSO years are identified in Rasmusson and Carpenter (1983). The years are generally those associated with the maximum positive sea surface temperature anomalies in the east Pacific.]

Region	Season	% Positive (Number positive/ Number of ENSOs)
	Precipitation	
Gulf and Mexican (GM)	Oct (0) to Mar (+)	81 (18/22)
Great Basin (GB)	Apr (0) to Oct (0)	81 (9/11)
	Temperature	
Northwest North American (NNA)	Dec (0) to Mar (+)	81 (17/21)
Southeast United States (SUS)	Oct (0) to Mar (+)	20 (5/25)

patterns may not be the same. The temperature response in North America can be related to the "teleconnections," i.e., the PNA circulation pattern, arising from low-latitude forcing of the midlatitude circulation. The precipitation response to ENSO may be more easily explained in terms of direct or shorter range effects related to the enhanced subtropical jet stream and warmer than normal Pacific Ocean water.

Acknowledgments. We wish to thank E. Rasmusson for suggesting the analysis approach and for his many helpful comments. The very useful concept of the "coherence" was developed from a suggestion by E. Epstein. The comments and suggestions of our other colleagues at the Climate Analysis Center, in particular, V. Kousky and P. Arkin, are likewise acknowledged. Comments by A. Douglas, Creighton University, and T. Karl, National Climate Data Center, helped to improve the paper. Thanks are also due to R. Jenne, W. Spangler, and D. Shea of NCAR for their assistance with the station data. J. Kopman provided valuable help in preparing the figures. This research was partially supported by Equatorial Pacific Ocean Climate Studies (EPOCS) funding.

REFERENCES

Arkin, P. A., 1982: The relationship between interannual variability in the 200 mb tropical wind field and the Southern Oscillation. *Mon. Wea. Rev.,* **110,** 1391–1404.

Berlage, H. P., 1966: The Southern Oscillation and world weather. *Meded. Verh.,* **88,** 152 pp. [Available from KNMI, P.O. 201, De Bilt, Netherlands.]

Blackmon, M. L., J. E. Geisler and E. J. Pitcher, 1983: A general circulation model study of January climate anomaly patterns associated with interannual variation of equatorial Pacific sea surface temperature. *J. Atmos. Sci.,* **40,** 1410–1425.

Douglas, A. V., and P. J. Englehart, 1981: On a statistical relationship between autumn rainfall in the central equatorial Pacific and subsequent winter precipitation in Florida. *Mon. Wea. Rev.,* **109,** 2377–2382.

——, and ——, 1984: Factors leading to the heavy precipitation regimes of 1982–83 in the United States. *Proc. Eighth Annual Climate Diagnostics Workshop,* Downsview, Ontario, 42–54. [NTIS PB84-192418.]

Horel, J. D., and J. M. Wallace, 1981: Planetary scale atmospheric phenomena associated with the Southern Oscillation. *Mon. Wea. Rev.,* **109,** 813–829.

Hoskins, B. J., and D. J. Karoly, 1981: The steady linear response of a spherical atmosphere in thermal and orographic forcing. *J. Atmos. Sci.,* **38,** 1179–1196.

Hsu, C. F., and J. M. Wallace, 1976: The global distribution of the annual and semiannual cycles in precipitation. *Mon. Wea. Rev.,* **104,** 1093–1101.

Janowiak, J. E., C. F. Ropelewski and M. S. Halpert, 1986: The precipitation anomaly classification: A method for monitoring regional precipitation deficiency and excess on the globe. *J. Climate Appl. Meteor.,* **25,** 565–574.

Kousky, V. E., M. T. Kagano and I. F. A. Cavalcanti, 1984: A review of the Southern Oscillation: Oceanic–atmospheric circulation changes and related rainfall anomalies. *Tellus,* **36A,** 490–502.

Meisner, B. N., 1976: A study of Hawaiian and Line Island rainfall. UHMET REP 76-4, Dept. Meteor., University of Hawaii, Honolulu, 182 pp.

National Climatic Data Center, 1981: *Divisional Normals and Standard Deviations of Temperature (°F) and Precipitation (Inches) 1931–1980, Climatography of the United States No. 85.* [Available from the National Climatic Data Center, Federal Building, Asheville, NC.]

Norton, J., D. McLain, R. Brainard and D. Husby, 1985: The 1982–83 El Niño event off Baja and Alta, California, and its ocean climate context. *El Niño North; Niño effects in the Eastern Subarctic Pacific Ocean,* Wooster and Fluharty, Eds. [Available from the Washington Sea Grant Program, College of Ocean and Fishery Sciences, University of Washington.]

Opsteegh, J. D., and H. M. van den Dool, 1980: Seasonal differences in the stationary response of a linearized primitive equation model: Prospects for long range forecasting? *J. Atmos. Sci.,* **37,** 2169–2185.

Rasmusson, E. M., and T. H. Carpenter, 1982: Variations in tropical sea surface temperature and surface wind fields associated with the Southern Oscillation/El Niño. *Mon. Wea. Rev.,* **110,** 354–384.

——, and ——, 1983: The relationship between eastern equatorial Pacific sea surface temperatures and rainfall over India and Sri Lanka. *Mon. Wea. Rev.,* **111,** 517–528.

——, and J. M. Wallace, 1983: Meteorological aspects of the El Niño/Southern Oscillation. *Science,* **222,** 1195–1202.

Ropelewski, C. F., 1986: North American precipitation patterns during winter and spring of 1982/83 in comparison to the typical El Niño/Southern Oscillation (ENSO) response. *Proc. First WMO Workshop on the Diagnosis and Prediction of Monthly and Seasonal Atmospheric Variations over the Globe,* College Park, WMO. [Available from the WMO World Climate Research Program, Case Postale No. 5, Ch-1211, Geneve 20, Switzerland.]

——, J. E. Janowiak and M. S. Halpert, 1985: The analysis and display of real-time surface climate data. *Mon. Wea. Rev.,* **113,** 1101–1106.

Shukla, J., and D. A. Paolino, 1983: The Southern Oscillation and long-range forecasting of the summer monsoon rainfall over India. *Mon. Wea. Rev.,* **111,** 1830–1837.

Walker, G. T., 1924: Correlation in seasonal variations of weather, IX: A further study of world weather. *Mem. Indian Meteor. Dept.,* **24,** 275–332.

——, and E. W. Bliss, 1932: World Weather V. *Mem. Roy. Meteor. Soc.,* **4,** 53–84.

Wallace and Gutzler, 1981: Teleconnections in the geopotential height field during Northern Hemisphere winter. *Mon. Wea. Rev.,* **109,** 784–812.

Webster, P. S., 1981: Mechanisms determining the atmospheric response to sea surface temperature anomalies. *J. Atmos. Sci.,* **38,** 554–571.